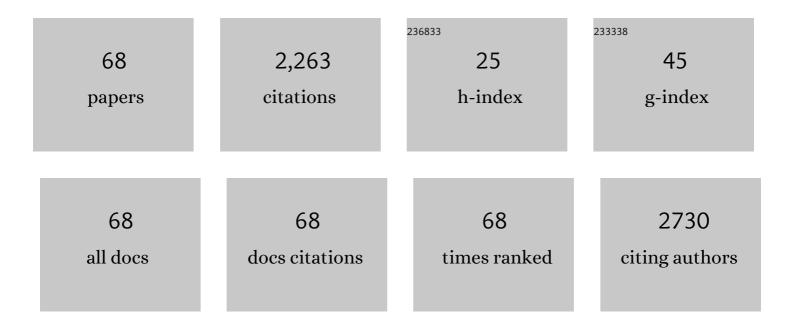
## Yoshitaka Bessho

List of Publications by Year in descending order

Source: https://exaly.com/author-pdf/2058720/publications.pdf Version: 2024-02-01



#	Article	IF	CITATIONS
1	Transposable element in fish. Nature, 1996, 383, 30-30.	13.7	211
2	Imaging live cell in micro-liquid enclosure by X-ray laser diffraction. Nature Communications, 2014, 5, 3052.	5.8	183
3	Ribozyme-catalyzed tRNA aminoacylation. Nature Structural Biology, 2000, 7, 28-33.	9.7	164
4	Insertion of a novel transposable element in the tyrosinase gene is responsible for an albino mutation in the medaka fish, Oryzias latipes. Molecular Genetics and Genomics, 1995, 249, 400-405.	2.4	103
5	Tertiary structure checkpoint at anticodon loop modification in tRNA functional maturation. Nature Structural and Molecular Biology, 2009, 16, 1109-1115.	3.6	97
6	Structural basis for functional mimicry of long-variable-arm tRNA by transfer-messenger RNA. Proceedings of the National Academy of Sciences of the United States of America, 2007, 104, 8293-8298.	3.3	96
7	Radiation and speciation of pelagic organisms during periods of global warming: the case of the common minke whale, Balaenoptera acutorostrata. Molecular Ecology, 2007, 16, 1481-1495.	2.0	83
8	Essentiality of threonylcarbamoyladenosine (t <sup>6</sup> <scp>A</scp> ), a universal t <scp>RNA</scp> modification, in bacteria. Molecular Microbiology, 2015, 98, 1199-1221.	1.2	72
9	Mitochondrial genes are found on minicircle DNA molecules in the mesozoan animal Dicyema 1 1Edited by J. Karn. Journal of Molecular Biology, 1999, 286, 645-650.	2.0	61
10	Translation of Synonymous Codons in Family Boxes byMycoplasma capricolumtRNAs with Unmodified Uridine or Adenosine at the First Anticodon Position. Journal of Molecular Biology, 1995, 251, 486-492.	2.0	57
11	Conservation of two distinct types of 100 <scp>S</scp> ribosome in bacteria. Genes To Cells, 2013, 18, 554-574.	0.5	56
12	Planarian mitochondria II. The unique genetic code as deduced from cytochrome c oxidase subunit I gene sequences. Journal of Molecular Evolution, 1992, 34, 331-335.	0.8	55
13	A tRNA aminoacylation system for non-natural amino acids based on a programmable ribozyme. Nature Biotechnology, 2002, 20, 723-728.	9.4	54
14	Aquifex aeolicus tRNA (N2,N2-Guanine)-dimethyltransferase (Trm1) Catalyzes Transfer of Methyl Groups Not Only to Guanine 26 but Also to Guanine 27 in tRNA. Journal of Biological Chemistry, 2009, 284, 20467-20478.	1.6	54
15	Crystal structure of archaeal tRNA(m <sup>1</sup> G37)methyltransferase aTrm5. Proteins: Structure, Function and Bioinformatics, 2008, 72, 1274-1289.	1.5	53
16	Crystal Structure of tRNA Adenosine Deaminase (TadA) from Aquifex aeolicus. Journal of Biological Chemistry, 2005, 280, 16002-16008.	1.6	49
17	Synthesis of Janus-Like Gold Nanoparticles with Hydrophilic/Hydrophobic Faces by Surface Ligand Exchange and Their Self-Assemblies in Water. Langmuir, 2015, 31, 4054-4062.	1.6	47
18	Structure of an archaeal TYW1, the enzyme catalyzing the second step of wye-base biosynthesis. Acta Crystallographica Section D: Biological Crystallography, 2007, 63, 1059-1068.	2.5	44

Yoshitaka Bessho

#	Article	IF	CITATIONS
19	Yolk/Shell Assembly of Cold Nanoparticles by Size Segregation in Solution. Journal of the American Chemical Society, 2016, 138, 3274-3277.	6.6	37
20	The Tyrosinase Gene from Medakafish: Transgenic Expression Rescues Albino Mutation. Pigment Cell & Melanoma Research, 1998, 11, 283-290.	4.0	35
21	Planarian mitochondria I. Heterogeneity of cytochrome c oxidase subunit I gene sequences in the freshwater planarian, Dugesia japonica. Journal of Molecular Evolution, 1992, 34, 324-330.	0.8	33
22	Crystal Structure of tRNA N2,N2-Guanosine Dimethyltransferase Trm1 from Pyrococcus horikoshii. Journal of Molecular Biology, 2008, 383, 871-884.	2.0	30
23	Lack of peptide-release activity responding to codon UGA inMycoplasma capricolum. Nucleic Acids Research, 1993, 21, 1335-1338.	6.5	29
24	Xâ€ray crystal structure of a hypothetical Sua5 protein from <i>Sulfolobus tokodaii</i> strain 7. Proteins: Structure, Function and Bioinformatics, 2008, 70, 1108-1111.	1.5	29
25	Crystal Structures of Tyrosyl-tRNA Synthetases from Archaea. Journal of Molecular Biology, 2006, 355, 395-408.	2.0	27
26	Evolving genetic code. Proceedings of the Japan Academy Series B: Physical and Biological Sciences, 2008, 84, 58-74.	1.6	27
27	Ribosomal protein L31 in <i>Escherichia coli</i> contributes to ribosome subunit association and translation, whereas short L31 cleaved by protease 7 reduces both activities. Genes To Cells, 2017, 22, 452-471.	0.5	27
28	Crystal structure of the probable haloacid dehalogenase PH0459 from Pyrococcus horikoshii OT3. Protein Science, 2006, 15, 373-377.	3.1	24
29	Life without tRNAArg–adenosine deaminase TadA: evolutionary consequences of decoding the four CGN codons as arginine in Mycoplasmas and other Mollicutes. Nucleic Acids Research, 2013, 41, 6531-6543.	6.5	24
30	Serial crystallography captures dynamic control of sequential electron and proton transfer events in a flavoenzyme. Nature Chemistry, 2022, 14, 677-685.	6.6	24
31	Crystal Structure of the RNA 2′-Phosphotransferase from Aeropyrum pernix K1. Journal of Molecular Biology, 2005, 348, 295-305.	2.0	23
32	Substrate tRNA Recognition Mechanism of a Multisite-specific tRNA Methyltransferase, Aquifex aeolicus Trm1, Based on the X-ray Crystal Structure. Journal of Biological Chemistry, 2011, 286, 35236-35246.	1.6	23
33	Crystal structure of hydrogenase maturating endopeptidase Hycl from Escherichia coli. Biochemical and Biophysical Research Communications, 2009, 389, 310-314.	1.0	21
34	Crystal structure of <i>sulfolobus tokodaii</i> sua5 complexed with <scp>L</scp> â€ŧhreonine and AMPPNP. Proteins: Structure, Function and Bioinformatics, 2011, 79, 2065-2075.	1.5	21
35	Structural Basis of the Initial Binding of tRNAlle Lysidine Synthetase TilS with ATP and L-Lysine. Structure, 2007, 15, 1642-1653.	1.6	20
36	The crystal structure of leucyl/phenylalanyl-tRNA-protein transferase from Escherichia coli. Protein Science, 2007, 16, 528-534.	3.1	20

Yoshitaka Bessho

#	Article	IF	CITATIONS
37	Crystal Structure and Mutational Study of a Unique SpoU Family Archaeal Methylase that Forms 2′-O-Methylcytidine at Position 56 of tRNA. Journal of Molecular Biology, 2008, 375, 1064-1075.	2.0	20
38	Crystal structure of human myo-inositol monophosphatase 2, the product of the putative susceptibility gene for bipolar disorder, schizophrenia, and febrile seizures. Proteins: Structure, Function and Bioinformatics, 2007, 67, 732-742.	1.5	18
39	Crystal structure and RNA-binding analysis of the archaeal transcription factor NusA. Biochemical and Biophysical Research Communications, 2007, 355, 122-128.	1.0	17
40	Characterization and Structure of the Aquifex aeolicus Protein DUF752. Journal of Biological Chemistry, 2012, 287, 43950-43960.	1.6	15
41	Crystal Structure of Methanocaldococcus jannaschii Trm4 Complexed with Sinefungin. Journal of Molecular Biology, 2010, 401, 323-333.	2.0	14
42	Adaptation of intronic homing endonuclease for successful horizontal transmission. FEBS Journal, 2005, 272, 2487-2496.	2.2	13
43	Crystal structures of possible lysine decarboxylases from Thermus thermophilus HB8. Protein Science, 2008, 13, 3038-3042.	3.1	11
44	Thermostable Mismatch-Recognizing Protein MutS Suppresses Nonspecific Amplification during Polymerase Chain Reaction (PCR). International Journal of Molecular Sciences, 2013, 14, 6436-6453.	1.8	11
45	Binding and Enhanced Binding between Key Immunity Proteins TRAF6 and TIFA. ChemBioChem, 2019, 20, 140-146.	1.3	11
46	Cloning of the Mycoplasma capricolum gene encoding peptide-chain release factor. Gene, 1996, 169, 101-103.	1.0	10
47	Crystal structure of the manganese transport regulatory protein from <i>Escherichia coli</i> . Proteins: Structure, Function and Bioinformatics, 2009, 77, 741-746.	1.5	10
48	Crystal structure of tRNA m1A58 methyltransferase TrmI from Aquifex aeolicus in complex with S-adenosyl-l-methionine. Journal of Structural and Functional Genomics, 2014, 15, 173-180.	1.2	9
49	XFEL coherent diffraction imaging for weakly scattering particles using heterodyne interference. AIP Advances, 2020, 10, .	0.6	9
50	Crystal structure of the bifunctional tRNA modification enzyme MnmC from <i>Escherichia coli</i> . Protein Science, 2011, 20, 1105-1113.	3.1	8
51	Human DNA Polymerase μ Can Use a Noncanonical Mechanism for Multiple Mn <sup>2+</sup> -Mediated Functions. Journal of the American Chemical Society, 2019, 141, 8489-8502.	6.6	8
52	Crystal Structure of the tRNA Pseudouridine Synthase TruA from Thermus Thermophilus HB8. RNA Biology, 2006, 3, 115-121.	1.5	7
53	Twist and turn: a revised structural view on the unpaired bubble of class II CPD photolyase in complex with damaged DNA. IUCrJ, 2018, 5, 608-618.	1.0	7
54	Crystal structure of the hypothetical protein TTHA1013 from Thermus thermophilus HB8. Proteins: Structure, Function and Bioinformatics, 2005, 61, 1117-1120.	1.5	6

#	Article	IF	CITATIONS
55	Crystal structure of a predicted phosphoribosyltransferase (TT1426) from Thermus thermophilus HB8 at 2.01 A resolution. Protein Science, 2005, 14, 823-827.	3.1	6
56	Structure of an archaeal homologue of the bacterial Fmu/RsmB/RrmB rRNA cytosine 5-methyltransferase. Acta Crystallographica Section D: Biological Crystallography, 2010, 66, 1301-1307.	2.5	6
57	Extending the potential of x-ray free-electron lasers to industrial applications—an initiatory attempt at coherent diffractive imaging on car-related nanomaterials. Journal of Physics B: Atomic, Molecular and Optical Physics, 2015, 48, 244008.	0.6	6
58	Phospho-Priming Confers Functionally Relevant Specificities for Rad53 Kinase Autophosphorylation. Biochemistry, 2017, 56, 5112-5124.	1.2	6
59	Complete Genome Sequence of Thermus thermophilus Strain HB5018, Isolated from Mine Hot Spring in Japan. Microbiology Resource Announcements, 2021, 10, .	0.3	5
60	Micro-liquid enclosure array and its semi-automated assembling system for x-ray free-electron laser diffractive imaging of samples in solution. Review of Scientific Instruments, 2020, 91, 083706.	0.6	4
61	Design of a liquid cell toward three-dimensional imaging of unidirectionally-aligned particles in solution using X-ray free-electron lasers. Physical Chemistry Chemical Physics, 2020, 22, 2622-2628.	1.3	3
62	Complete Genome Sequences of Thermus thermophilus Strains HB5002 and HB5008, Isolated from Mine Hot Spring in Japan. Microbiology Resource Announcements, 2021, 10, .	0.3	3
63	Development of Multilayer Focusing Mirror System for XFEL CDI Experiments of Biological Particles. Microscopy and Microanalysis, 2018, 24, 298-299.	0.2	2
64	Vibrio cholerae biofilm scaffolding protein RbmA shows an intrinsic, phosphateâ€dependent autoproteolysis activity. IUBMB Life, 2021, 73, 418-431.	1.5	2
65	Femtosecond X-ray Laser Reveals Intact Sea–Island Structures of Metastable Solid-State Electrolytes for Batteries. Nano Letters, 2022, 22, 4603-4607.	4.5	2
66	Crystal structure of the MazG-related nucleoside triphosphate pyrophosphohydrolase from Thermotoga maritima MSB8. Journal of Structural and Functional Genomics, 2015, 16, 81-89.	1.2	1
67	Coherent Imaging Using SACLA. Nihon Kessho Gakkaishi, 2017, 59, 18-23.	0.0	0
68	Nano-Imaging Under Controlled Environment Using SACLA. The Review of Laser Engineering, 2017, 45, 508.	0.0	0